A Multichannel Cloud Pyranometer System for Airborne Measurement of Solar Spectral Reflectance by Clouds

SHOJI ASANO AND MASATAKA SHIOBARA

Meteorological Research Institute, Tsukuba, Japan

YUJI NAKANISHI* AND YUKIHARU MIYAKE

EKO Instrument Company, Hatagaya, Tokyo, Japan

(Manuscript received 21 February 1994, in final form 8 November 1994)

ABSTRACT

The design and performance of a spectral radiometer system are described for airborne measurements of solar flux reflectance by clouds. The system consists of a pair of identical multichannel pyranometers: one installed on the top and the other on the bottom of an aircraft fuselage to measure the downward and upward solar irradiances, respectively. This measurement scheme has an advantage in that reflectances derived from ratios between the upward and downward irradiances can avoid the need for absolute radiometric calibrations. The multichannel cloud pyranometer (MCP) system measures near-monochromatic solar irradiances at nine discrete wavelengths between 420 and 1650 nm by using interference filters with very narrow bandwidths. Included among these wavelengths are 760 and 938 nm in the oxygen and water vapor absorption bands, respectively. Solar radiation passing through the filters is instantly detected by a silicon photodiode for wavelength $\lambda < 1$ μm and by a germanium photodiode for $\lambda > 1$ μm. Good performance of the MCP system was confirmed through laboratory calibrations and airborne tests. The MCP system is suitable for remote sensing application to retrieve cloud physical parameters of water clouds from airborne spectral reflectance measurements.

1. Introduction

Radiative properties of clouds are related in a complicated manner to both their microphysical and macrophysical structures. To advance a better understanding of the relationship between the solar radiative properties of clouds and their microphysical structure, it is very useful to study the spectral characteristics of the solar radiation reflected, transmitted, and/or absorbed by the clouds. On the other hand, the possibility of using solar spectral reflection measurements to derive cloud characteristics (optical thickness, particle size, phase, etc.) has long been recognized (e.g., Hansen and Pollack 1970; Twomey 1971). Recently, various types of airborne spectral radiometers have been developed and applied to the remote sensing of cloud characteristics. Among others, some examples are the National Aeronautical and Space Administration (NASA) multichannel scanning radiometer discussed by Curran et al. (1981) and King (1987), the NASA cloud absorption radiometer by King et al. (1986), the Commonwealth Science and Industrial Research Organisation (CSIRO) spectral radiometer (SPERAD) by Scott and Stephens (1984) and Stephens and Scott (1985), a scanning radiometer by Cocks et al. (1983), and the United Kingdom Meteorological Office multichannel radiometer by Rawlins and Foot (1990). Some of these radiometers were designed to measure the spectral radiance over a narrow field of view and were used to obtain the bidirectional reflectivity of clouds. On the other hand, the radiometer by Cocks et al. (1983) and the CSIRO SPERAD were designed to measure the narrow-angle nadir radiance as well as the downward solar irradiance, by using a calibrated diffuser, and used to obtain the bidirectional reflectance for water clouds (Twomey and Cocks 1989; Stephens and Platt 1987).

A great advantage in the measurement of flux reflectance rather than narrow-angle radiance is that absolute radiometric calibrations of the instrument are not necessary. Also, when compared with theoretical calculations and remote sensing analyses, complicated and extensive calculations of the observational angle dependence and scattering phase-function dependence of reflected radiance can be avoided. On the other hand, the spatial resolution of the flux measurement may be lower than that of the radiance measurement, because the upward radiative flux reflected by clouds is composed of radiation scattered from a wider cloud region.

We have developed a spectral radiometer system with easy handling in airborne and ground-based use.

* Current affiliation: Nakanishi Tech, Akikawa, Tokyo, Japan.

Corresponding author address: Shoji Asano, Meteorological Research Institute, Nagamine, Tsukuba, Ibaraki 305, Japan.

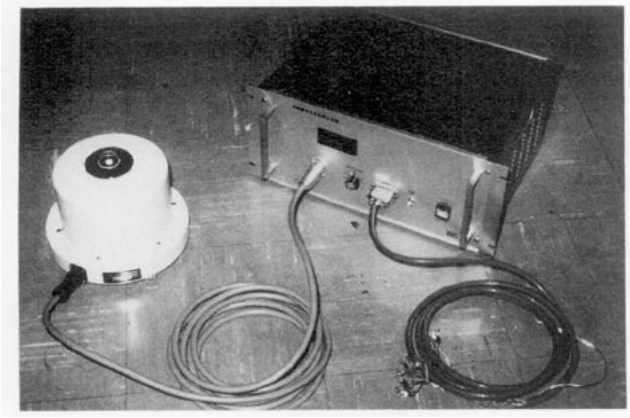

FIG. 1. Photograph of a set of MCP: on the left the sensor, on the right the controller.

Motivation for the development of the instrument was focused on the need to

(i) obtain high-quality observational data of spectral solar irradiances, which are usable to validate monochromatic radiative-transfer calculations, over a wide region of wavelength from visible to the near-infrared, and

(ii) apply the system to the remote sensing of cloud physical parameters such as optical thickness, geometrical thickness, effective particle radius, and phase of cloud particles from airborne spectral reflectance measurements.

In this paper, we shall describe the design and performance of the spectral radiometer system for measuring spectral flux reflectances in the visible and near-infrared region. The application of the radiometer to remote sensing of cloud physical parameters will be a major theme of a separate paper (Asano et al. 1995).

2. Description of instrument

A spectral radiometer system has been developed for airborne measurements of solar spectral reflectance from clouds. This system consists of a pair of multichannel pyranometers, with one installed on the top and the other on the bottom of an aircraft fuselage to measure the downward and upward solar spectral irradiances, respectively. The pyranometer system is termed the multichannel cloud pyranometer, or abbreviated as the MCP system. Figure 1 shows a photograph of the MCP set for measuring the downward solar irradiance. Another identical set is used for measuring upward irradiance.

The MCP system is designed to measure quasi-monochromatic solar irradiances at nine selected discrete wavelengths. To determine the channel wavelengths, extensive radiative transfer calculations were carried out for solar reflectance and transmittance of various water and ice cloud models. Nine wavelengths were selected that represent the characteristic spectral features over a wide spectral region between 420 and 1650 nm. The wavelength region was limited by the spectral responses of the detectors used, which will be described later. The MCP channels are specified by using narrowband interference filters. Table 1 summarizes the characteristics of the interference filters that were installed in the MCP pair for measuring the downward and upward solar irradiances. Among the nine channels, two were chosen at wavelengths of 760 and 938 nm for the molecular oxygen absorption band and water vapor absorption band, respectively. The other seven channels were selected for the so-called window regions, where gaseous absorption can be neglected.

We have proposed a remote sensing algorithm to retrieve various cloud-physical parameters of water clouds from the solar reflectances measured by the MCP system at four wavelengths of 500, 938, 760, and 1650 nm (Asano and Shiobara 1993). The estimation assumes a locally plane-parallel and vertically homogeneous water-cloud layer with monomodal particle size distributions. The visible optical thickness and the effective particle radius of the water-cloud layer can be simultaneously retrieved from the MCP reflectances

TABLE 1. Characteristics of interference filters.

Channel/ wavelength (nm)	ES84 (downward flux)			ES85 (upward flux)		
	Band-center wavelength (nm)	Transmission at band center (%)	Half-transmission bandwidth (nm)	Band-center wavelength (nm)	Transmission at band center (%)	Half-transmission bandwidth (nm)
1/420	421.3	26.8	3.0	421.0	28.0	3.0
2/500	500.2	48.4	3.0	500.0	47.0	3.0
3/675	676.8	37.0	2.3	676.0	38.0	3.0
4/760	760.3	41.0	2.0	760.5	46.0	2.0
5/862	863.0	53.0	3.5	863.0	52.0	3.0
6/938	936.5	38.0	3.0	937.0	40.5	3.0
7/1080	1078.0	45.6	4.0	1080.5	49.0	3.5
8/1225	1224.0	52.9	4.2	1226.0	53.0	4.0
9/1650	1652.0	46.9	4.3	1651.0	46.5	4.0

measured at the visible channel of 500 nm and at the near-infrared channel of 1650 nm. The estimation procedure is similar to the idea proposed by Twomey and Cocks (1989) and Nakajima and King (1990). The liquid water content can then be retrieved from the MCP reflectance at the oxygen absorption band channel centered at 760 nm. Finally, the in-cloud water vapor amount can then be estimated from the MCP reflectance at the water vapor absorption band channel of 938 nm. Using these directly retrieved parameters, we can estimate byproduct parameters such as integrated liquid water path, cloud particle concentration, and geometrical thickness of the homogeneous cloud layer. The retrieval method was applied to the MCP spectral reflectance data obtained through aircraft observations for stratocumulus clouds. Reasonable values of the cloud physical parameters were successfully retrieved for the stratocumulus clouds. More detailed discussion is the subject of a separate paper (Asano et al. 1995).

Figure 2 shows a schematic illustration of the cross-sectional view of the MCP sensor. After passing through the fused quartz dome (a), solar radiation incident on the diffuser (b) is scattered by the diffuser and converted to completely diffused radiation. Its intensity at the bottom of the diffuser is proportional to that of the incident solar irradiance. The transmitted diffuse radiation is converted to quasi-monochromatic light after passing through one of the narrowband interference filters (c), which are installed in the filter wheel (g). The filter wheel can accommodate nine interference filters and one blind filter and rotates at a speed of 300 rpm (5 Hz). The channel position can be identified by the photo-interrupter (h) that detects the filter position.

The quasi-monochromatic radiation transmitted through the interference filter is then split into two detectors (e and f) by the silicon crystal beam splitter (d). Radiation consisting of wavelengths less than 1 μm (channels 1–6) is detected by a silicon photodiode (e), while radiation of wavelengths longer than 1 μm (channels 7–9) is detected by a germanium photodiode (f). The distances between the diffuser and the interference filter and between the filter and the detectors are taken large enough so that incidence of the detected radiation on the filter becomes almost perpendicular to the filter plane, in order to minimize a band-center-wavelength shift. In this configuration, the maximum incidence angle is 6°, and the caused wavelength shift is much smaller than the corresponding bandwidth. In addition, the other component parts built in the MCP sensor are coated with a black nonglossy paint to avoid extra reflection and stray light.

The spectral responses of the silicon photodiode (Hamamatsu-Photonics, S1336-8BQ) and germanium photodiode (Hamamatsu-Photonics, B1919-01) are shown in Fig. 3. In the figure, the band-center wavelengths of the MCP channels are also indicated. Generally, interference filters and photodiodes may be dependent on temperature. To minimize temperature effects, the MCP sensor is temperature controlled at 35°C ± 1°C by use of the film heater (i).

Output signals from the two detectors are respectively amplified by the current-to-voltage amplifiers and converted to currents between 4 and 20 mA and then transferred to the controller unit. The signals are in time series, as shown by the lines Si and Ge in Fig. 4. On these lines, rectangular forms schematically represent the detected signals, corresponding to each interference filter (or MCP channel) and the blind filter (b on Si and b' on Ge). Appreciable signals from the blind filter channel represent zero-point drift of output from the detectors and amplifiers.

A sample-and-hold circuit is employed to separate the time serial signals into parallel signals from each channel. The controller unit contains nine independent sample-holder circuits. The ith channel signal, corrected for the zero drift of the corresponding detector measured as the blind filter signal, is held in the ith sample holder during one cycle of the filter wheel rotation. The signal is then converted and amplified to a direct current voltage between 0 and 10 mV, and its analog voltage can be transmitted in parallel with other channel output signals. Combined with the rapid rotation of the filter wheel at 5 Hz, and quick response of the detectors on the order of microseconds, this scheme yields almost coincident data among the different MCP channels. Further, an electronic smoothing is added to diminish noise from the detectors and amplifiers. The ultimate response time of the MCP system is designed to be 0.3 s in e-folding time, that is, a time constant of 63% ($=1 - e^{-1}$) rise for a square-wave input.

This response time is much faster than the time variations of the aircraft attitudes such as pitch, roll, and yaw that have a typical cycle on the order of several seconds. These fluctuations can strongly influence aircraft measurements of the downward solar irradiance on the horizontal plane. Assuming that the MCP system can instantly respond to aircraft attitude, the correction method proposed by Asano and Shiobara (1989) was employed for the tilt of the pyranometer plane due to aircraft attitude variations. The method evaluates the tilt angle of the pyranometer plane from the horizon by using the aircraft attitude data for angles of pitch, roll, and yaw as well as the heading azimuth. Then, a correction for the tilt is applied only to the direct component of the downward solar radiation, assuming that the diffuse component is isotropic and the ratio of diffuse to direct radiation is known.

3. Definitions of calibration and measurement

Radiometric calibration was obtained by observing a standard lamp. A 100-V, 500-W halogen–tungsten standard lamp was directly observed at a specified dis-

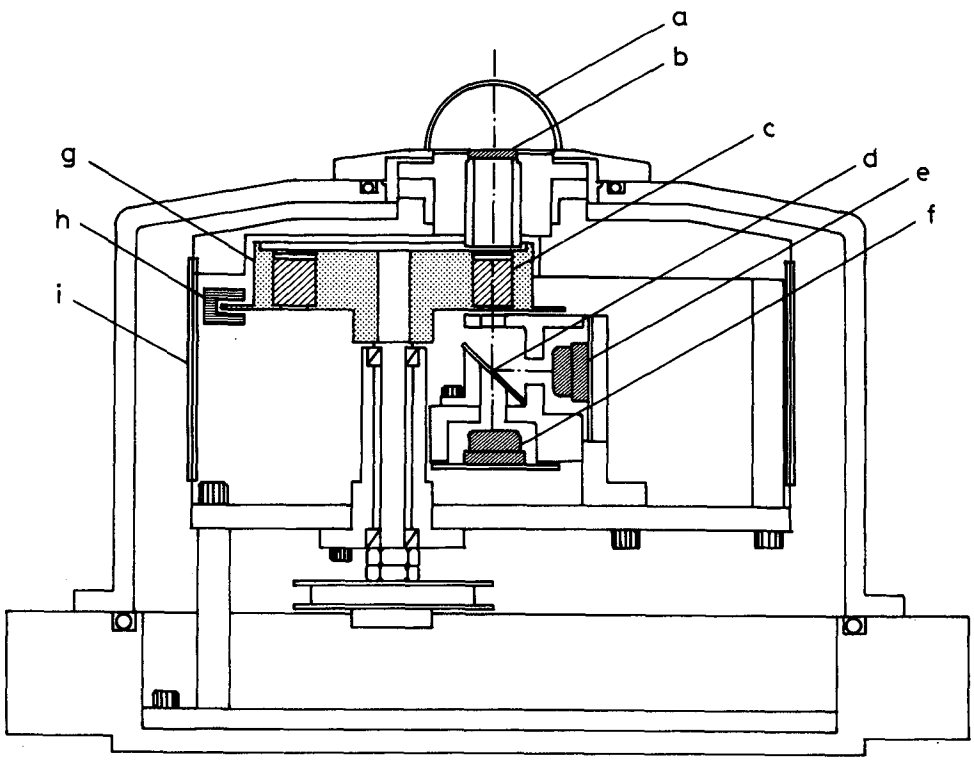

FIG. 2. Schematic illustration of the cross-sectional view of the MCP sensor, where a is the fused quartz dome, b the diffuser, c the interference filter, d the beam splitter, e the Si photodiode, f the Ge photodiode, g the filter wheel, h the optical sensor for filter position detection, and i the film heater.

tance. The lamp has been calibrated against the standard spectral irradiance of the Japan Electronic Instrument Calibration Center to better than 3% for the spectral region. The MCP system was calibrated by measuring its output voltage in each channel against the spectral irradiance of the lamp. The accuracy of this absolute calibration was estimated to be about 5%. The linearity of the MCP output was also examined by changing the distances between the MCP sensor and the standard lamp. This procedure proved that the MCP system has a good linearity performance.

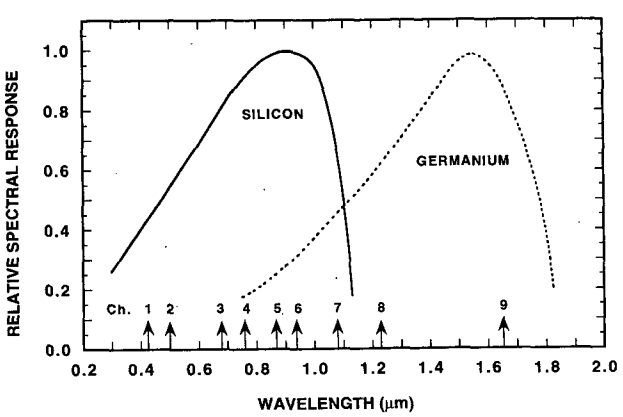

FIG. 3. Relative spectral responses of silicon photodiode (Hamamatsu-Photonics, S1336-8BQ) and germanium photodiode (Hamamatsu-Photonics, B1919-01), normalized by wavelengths of 0.9 and 1.55 μm, respectively. Positions of the MCP channels are indicated by the arrows on the abscissa.

For aircraft measurements of spectral reflectance using the MCP system, the relative calibration of the MCP pair is sufficient, as opposed to the absolute calibration. Here, relative calibration means a comparison of the output voltages versus the same incident irradiance of the MCP pair for measuring the downward and upward solar irradiances. In this case, solar radiation, rather than a standard lamp, is the better light source, since there might be some differences in setting the lamp and the MCP sensors.

Figure 5 shows an example of the results of a field comparison of the output voltages of the MCP pair, placed horizontally side by side, made during a day for channels 2 (500 nm), 4 (760 nm), 6 (938 nm), and 9 (1650 nm). The output voltages for each channel of the MCP pair are proportional to each other under the normal range of solar irradiance. The near-infrared channels detected by the germanium photodiode have slightly larger electrical noises, specially for low output voltages, than the channels by the silicon detector (see Fig. 5d). In practice, however, the proportional relationship between the output voltages of the MCP pair

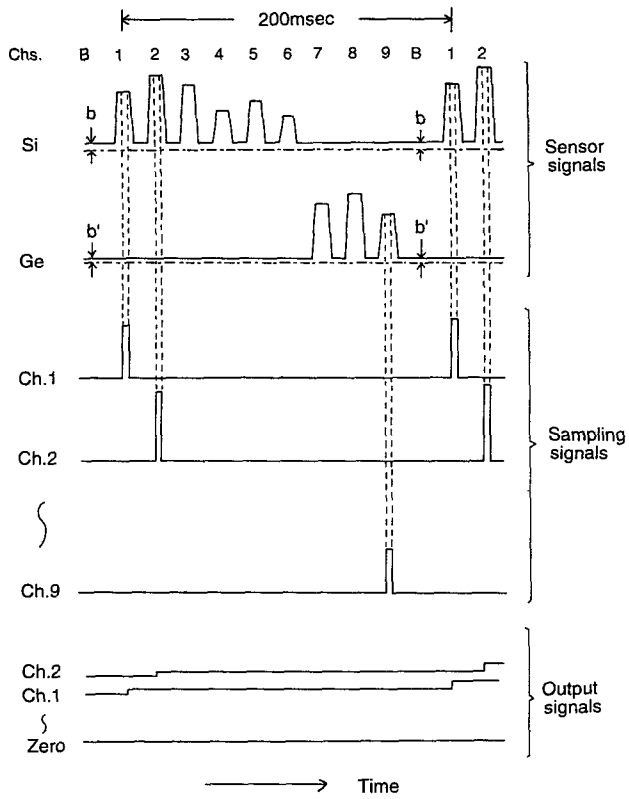

FIG. 4. A schematic time chart displaying the detector signals, sampling signals, and output signals. The lines denoted by Si and Ge indicate detector signals from the silicon photodiode and germanium photodiode, respectively. The dot–dash lines indicate zero levels of the detector output. The Si and Ge zero drifts are exaggerated and indicated by b and b' at the blind filter position B, respectively. The lines denoted by channel i are sampling signals, each corrected for zero drift, for the ith channel. The bottom lines represent output signals from the sample-holder circuits.

appears satisfactory for all the channels, with very good correlation.

Good performance of the incident angle dependence, or the so-called cosine response, is another important requirement for accurate measurements of horizontal irradiances. The cosine response was assessed by performing a calibration experiment at the radiometer calibration facility of the Japan Meteorological Agency (JMA). Figure 6 shows the cosine responses of the MCP pair for measuring the (a) downward and (b) upward solar irradiances, respectively. In the figures, the ordinates indicate the deviations $\mathrm{Er}(\theta)$ from the true cosine response, defined by the relation $\mathrm{Er}(\theta) = 1 - F(\theta)(F_0 \times \cos\theta)^{-1}$, where $F(\theta)$ and F_0 are the output voltages at the incident zenith angles θ and $\theta = 0$, respectively. The curves represent the mean errors $\mathrm{Er}(\theta)$ averaged over four azimuthal dependence calibrations made at every 90° azimuthal direction for each zenith angle. The azimuth-angle dependence is different for different channels and incident zenith angles. Generally, the dependence is larger for larger incident zenith angles, and the standard deviation of the four azimuthal calibrations reaches a channel-mean value of about 0.02 at $\theta = 70°$, increasing from negligibly small values for near-normal incidences of $\theta < 20°$. These figures reveal that the MCP system follows a true cosine response within 3% for incident zenith angles less than 70° with a mean uncertainty of ±1% due to the azimuth-angle dependence.

The cosine responses were taken into account for airborne measurements of the solar spectral reflectance by clouds. Assuming that the downward solar radiation over a cloud layer is almost completely composed of the direct solar beam, the correction compensating the azimuthally averaged cosine response shown in Fig. 6a is applied, as a function of the solar zenith angle, to the measured downward irradiance at each MCP channel. While, for the upward irradiance, the measured irradiance at all the MCP channels except channel 9 is simply increased by 1%, assuming that the upward radiation reflected by clouds is almost isotropic. For the upward irradiance at channel 9, no correction is applied for the cosine response. Taking into account these corrections and the characteristics of the MCP system, the ultimate errors involved in the airborne spectral reflectance measurements can be estimated as being, at most, 3%–4% for the solar zenith angles less than 70°.

4. In-flight performance

In-flight performance of the MCP system was tested through aircraft observations of stratocumulus clouds on 24 December 1986 and 20–21 September 1987. The MCP system was flown on board a Cessna 404 as one of a group of instruments that included upward- and downward-viewing pyranometers and pyrgeometers, an airborne video optical microscope (AVIOM) for measuring cloud particles, a Johnson–Williams (J–W hereafter) hot-wire device for liquid water content, and an air sampler system for measuring cloud-interstitial aerosols (MRI 1992). The AVIOM device was developed by the Meteorological Research Institute (MRI) cloud physics group (Tanaka et al. 1989). The MCP sensors for measuring the downward and upward spectral irradiances were installed on the top mount and the bottom mount of the aircraft fuselage, respectively. On the mounts, a pair of conventional pyranometers (EKO MS-801) were also installed for measuring the broadband total solar irradiances, a pair of pyranometers (EKO MS-801 with a RG715-cutoff filter dome) for the near-IR solar irradiance, and a pair of pyrgeometers (Eppley PIR) for measuring the longwave radiation. Figure 7 shows a photograph of the radiometer mounts installed on the top and bottom of the Cessna 404 fuselage. Pyranometers for measuring the broadband total and near-IR solar radiation, the Epply PIR, and the MCP sensors were installed in order, from the front to the rear.

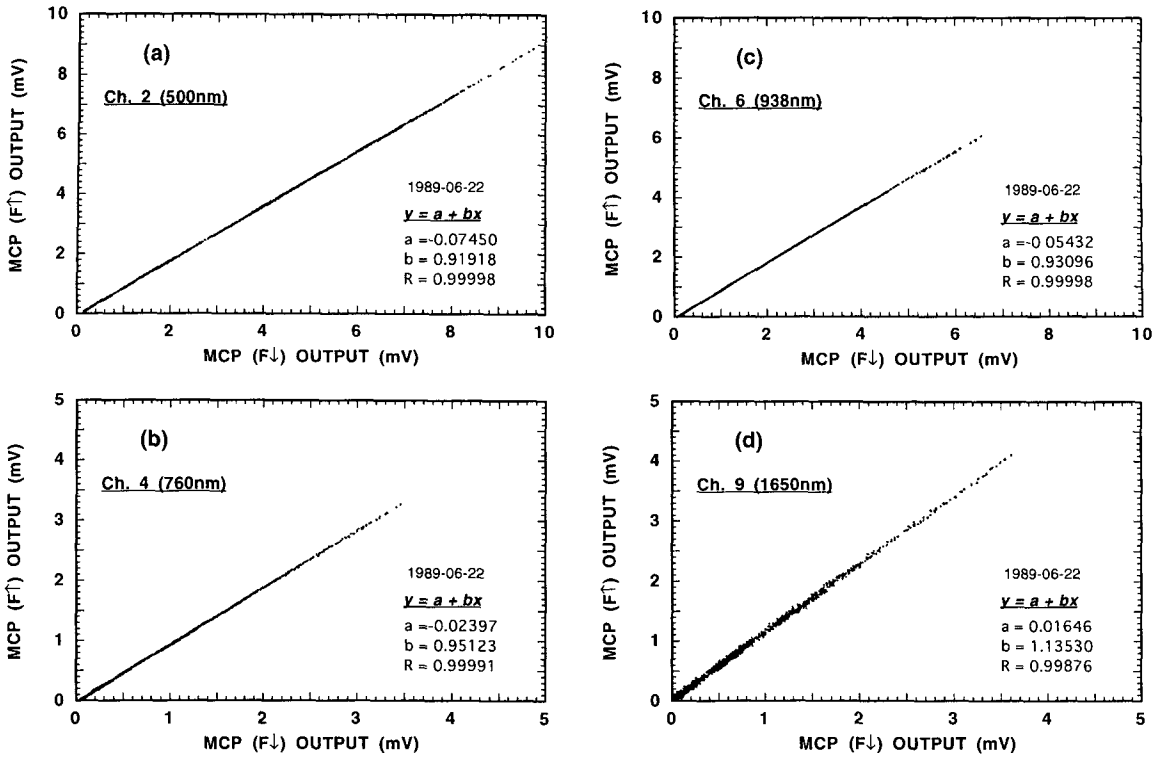

FIG. 5. Linear relationships between output signals from the MCP measuring the downward [MCP($F\downarrow$)] and upward [MCP($F\uparrow$)] fluxes. The data were obtained over a day-long period of comparative measurements. The coefficients a and b of the linear regression $y = a + bx$ of the data and their correlation coefficient R against the linear relationship are shown on each panel. In the linear regression, the variables x and y represent the simultaneous output voltages of the MCP($F\downarrow$) and MCP($F\uparrow$), respectively. (a) Channel 1 (500 nm), (b) channel 4 (760 nm), (c) channel 6 (938 nm), and (d) channel 9 (1650 nm).

Figure 8 shows an example of cloud reflectance values measured by the MCP system for channels 2 (500 nm), 4 (760 nm), 6 (938 nm), and 9 (1650 nm) during a level flight over a stratocumulus cloud layer observed on 20 September 1987. The cloud system was maritime stratocumulus accompanied by small patches of cumulus clouds scattered below the stratocumulus layer, between the levels of 800 and 1100 m. The observed top and base heights of the stratocumulus layer were estimated as 2700 and 2000 m, with an apparent thickness of 700 m. Radiation data were sampled every second (1 Hz). One minute along the abscissa is nearly equivalent to a horizontal distance of 5 km at a flight speed of about 80 m s^{-1}.

The spectral flux reflectance is defined here by the ratio of the upward radiative flux to the downward radiative flux measured at each channel of the MCP system during a level flight over a cloud layer. The reflectance defined in this manner is an apparent cloud reflectance that includes the effects due not only to cloud reflection, but also atmospheric scattering and absorption, and the underlying surface reflection. However, if the reflectance measurement is made just above the cloud layer, which is not so optically thin as to be significantly affected by the underlying surface reflection, the measured reflectance can represent the true cloud reflection. For the case shown in Fig. 8, the aircraft reflectance measurements were made during a level flight about 300 m above the stratocumulus layer. The figure shows highly fluctuating features in the time series distribution, revealing the horizontally inhomogeneous structure of the cloud system.

Figure 9 shows the wavelength distributions of the MCP-measured reflectances of the stratocumulus cloud system on 20 September 1987. The measured reflectances are the averaged values over the 1-min horizontal leg A, shown in Fig. 8. In the figure, the mean broadband cloud reflectances for the visible (denoted VIS) and near-infrared (NIR) regions are also indicated on the right ordinate axis, with values of 0.61 and 0.58, respectively. The near-IR broadband reflectance was measured by the near-IR pyranometers. The visible reflectance was obtained from the broadband visible solar irradiance, which was determined as differences between the total and near-IR solar irradiances. The good agreement among the MCP spectral reflectances and the independently measured broadband reflectances in the visible and near-IR regions indicates a reliable performance of the MCP system for airborne spectral reflectance measurements.

In the Fig. 9, the measured reflectances are also compared with theoretically simulated reflectances

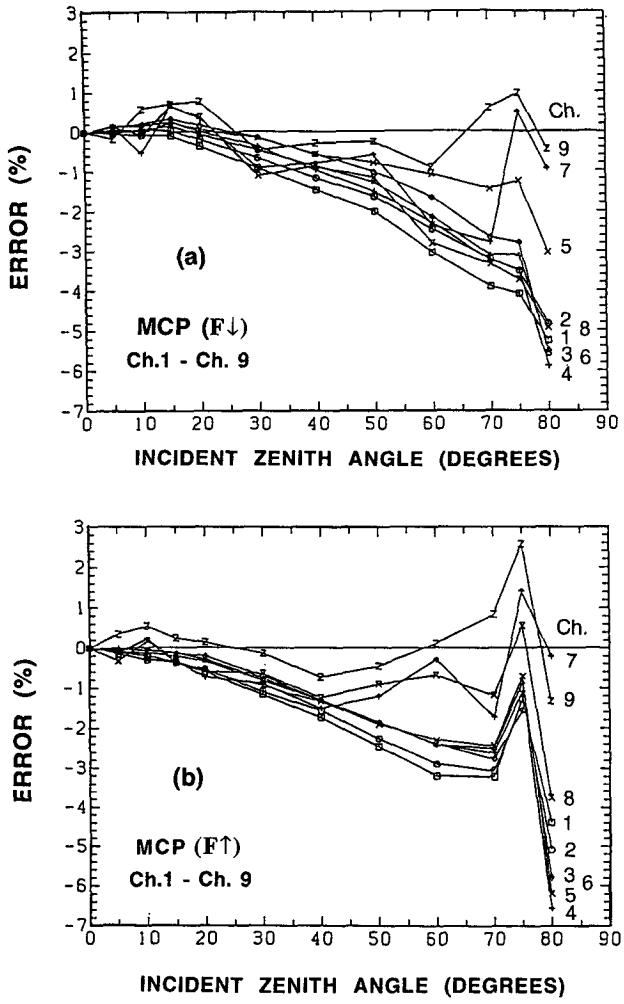

FIG. 6. Incident angle (cosine response) characteristics of the MCP. Panel (a) is for the MCP system for measuring the downward solar irradiance, and panel (b) is for the MCP system for measuring the upward irradiance. The curves represent mean deviations from a true cosine response, averaged over four azimuth-angle-dependence calibrations done at every 90° in the azimuth.

computed at the MCP channel wavelengths. Assuming a plane-parallel, homogeneous cloud layer, radiative transfer calculations were carried out by the doubling–adding method. Single-scattering properties of cloud particles were calculated from the Mie theory by employing optical constants of liquid water compiled by Hale and Qurrey (1973). Gaseous absorption due to oxygen molecules in channel 4 (760 nm) and water vapor in channel 6 (938 nm) was taken into account using the method of exponential sum fitting of transmission (Asano and Uchiyama 1987) for gaseous transmission functions averaged over the slit functions of the corresponding interference filters.

For the simulation calculations, the cloud was assumed to be a homogeneous layer having a liquid water content of 0.1 g m^{-3}. This was a mean value measured by the J–W hot-wire device during a level flight at 1326–1336 in the middle of the stratocumulus layer, prior to the reflectance measurements. The in-cloud water vapor amount was assumed to 7 g m^{-3}, the saturation vapor amount at the cloud-top temperature of 6°C. The cloud particle size distribution was measured by the AVIOM device, which produced a mean concentration of 190 cm^{-3} and an effective particle radius of 18 μm. The latter value appears to be overestimated due to uncertain calibrations in the particle sizing by the AVIOM device at the time of the observations (Tanaka et al. 1989).

Therefore, a lognormal distribution with an effective particle radius of 9 μm and an effective variance of 0.13 was assumed as the cloud particle size distribution in the Mie scattering calculations. The effective particle radius of 9 μm as well as an visible optical thickness of 16 were estimated as optimal mean values for the flight leg *A* from the remote sensing analysis of the MCP spectral reflectances at 500 and 1650 nm. The visible optical thickness and effective particle radius can be simultaneously determined from the MCP-measured reflectances of the visible channel of 500 nm and the near-IR channel of 1650 nm (Asano et al.

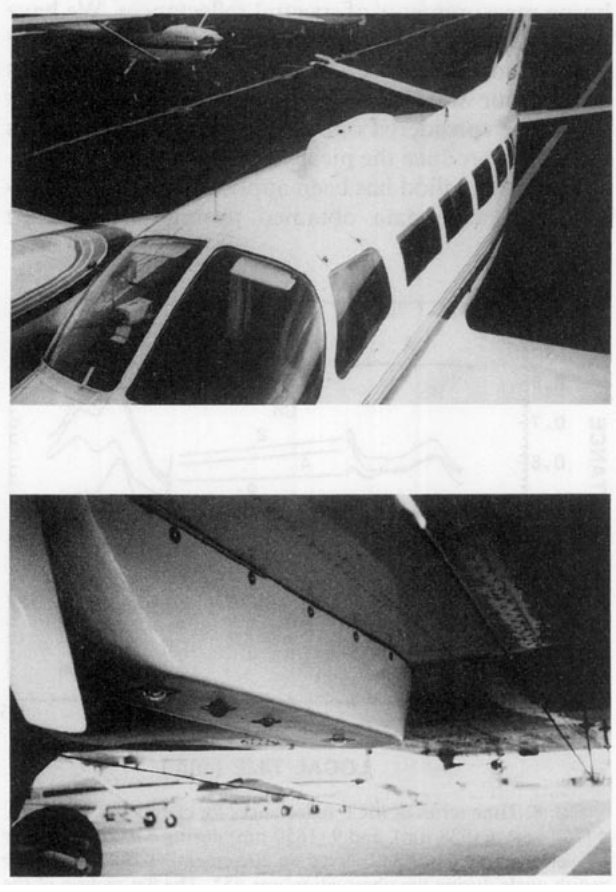

FIG. 7. Photograph of the radiometer mounts installed on the top and bottom of the Cessna 404 fuselage.

1995). Figure 9 illustrates a good agreement between the wavelength distribution of cloud reflectances measured by the MCP system and the theoretically simulated spectral distribution. This reveals that the MCP system can measure reasonable spectral reflectances in the wide wavelength region. It also suggests applicability of the present MCP system to the remote sensing of cloud physical parameters.

5. Concluding remarks

A spectral radiometer system has been developed for airborne measurements of solar spectral reflectances from clouds. The system consists of a pair of MCPs to measure the downward and upward solar irradiances. Good performance of the MCP system was confirmed through laboratory calibrations and airborne tests.

Airborne measurements of flux reflectance rather than narrow-angle radiance have the advantage that absolute radiometric calibration of the instrument can be avoid. However, identity of the spectral characteristics, especially, in the band-center wavelengths and bandwidths between the MCP pair is critically important for accurate spectral reflectance measurements.

One of the scientific interests is an application to remote sensing of cloud-physical parameters from airborne measurements of spectral reflectances. We have proposed a method to retrieve various cloud physical parameters of water clouds from the solar reflectances at the four wavelengths. The estimated parameters should be considered optically equivalent parameters that can reproduce the measured cloud radiative properties. The method has been applied to the MCP spectral reflectance data obtained through the aircraft

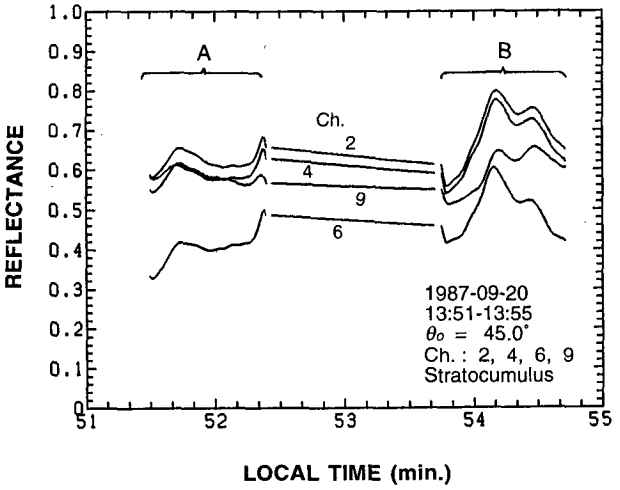

FIG. 8. Time series of MCP reflectances for channels 2 (500 nm), 4 (760 nm), 6 (938 nm), and 9 (1650 nm) during a level flight over a layer of stratocumulus observed on 20 September 1987. The solar zenith angle during the observation was 45°. The flat section of the curves between the regions A and B represents a no-data region during a turn of the aircraft.

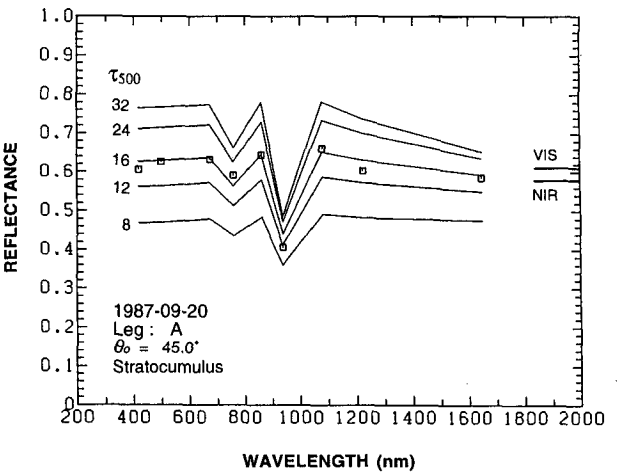

FIG. 9. Wavelength distribution of the measured MCP reflectances (open squares) averaged over the horizontal leg A, shown in Fig. 8. The bars denoted VIS and NIR on the right ordinate axis indicate the measured broadband reflectances in the visible and near-IR regions, respectively. Theoretically simulated spectral reflectances (solid lines) are shown for comparison for homogeneous water clouds with an effective particle radius of 9 μm and for different optical thicknesses τ_{500} at 500 nm of 8, 12, 16, 24, and 32.

observations for wintertime stratocumulus clouds done in the Western North Pacific Cloud-Radiation Experiment/MRI program (MRI 1992). The result is discussed in detail in a separate paper (Asano et al. 1995).

Acknowledgments. We would like to express our sincere thanks to the JMA radiometer calibration facility for assistance in the calibration experiments. Thanks are extended to Drs. T. Tanaka and M. Ikegami of the MRI and the Showa Aviation Co. for their helpful cooperation during the aircraft tests. We also thank anonymous reviewers for their suggestions for improvement of the paper.

REFERENCES

Asano, S., and A. Uchiyama, 1987: Application of an extended ESFT method to calculation of solar heating rates by water vapor absorption. *J. Quant. Spectrosc. Radiat. Transfer,* **38,** 147–158.

——, and M. Shiobara, 1989: Aircraft measurements of the radiative effects of tropospheric aerosols: I. Observational results of the radiative budget. *J. Meteor. Soc. Japan,* **67,** 847–861.

——, and ——, 1993: Estimation of cloud-physical parameters from solar spectral reflectance measurements. *Extended Abstracts, Int. WCRP Symp.—Clouds and Ocean in Climate,* Nagoya, Japan, Nagoya University, 7.22–7.25.

——, ——, and A. Uchiyama, 1995: Estimation of cloud-physical parameters from airborne solar spectral reflectance measurements for stratocumulus clouds. *J. Atmos. Sci.,* submitted.

Cocks, T. D., S. Dujmovic, W. D. King, and S. Twomey, 1983: Aircraft experiments in remote sensing of cloud properties. Preprints, *Fifth Symp. on Meterological Observations and Instrumentation,* Toronto, Ontario, Canada, Amer. Meteor. Soc., 169–173.

Curran, R. J., H. L. Kyle, L. R. Blaine, J. Smith, and T. D. Clem, 1981: Multichannel scanning radiometer for remote sensing cloud physical parameters. *Rec. Sci. Instrum.*, **52,** 1546–1555.

Hale, G. M., and M. R. Qurrey, 1973: Optical constants of water in the 200 nm to 200 mm wavelength region. *Appl. Opt.*, **12,** 555–563.

Hansen, J. E., and J. B. Pollack, 1970: Near-infrared light scattering by terrestrial cloud. *J. Atmos. Sci.*, **27,** 265–281.

King, M. D., 1987: Determination of the scaled optical thickness of clouds from reflected solar radiation measurements. *J. Atmos. Sci.*, **44,** 1734–1751.

——, M. G. Strange, P. Leone, and L. R. Blaine, 1986: Multiwavelength scanning radiometer for airborne measurements of scattered radiation within clouds. *J. Atmos. Oceanic Technol.*, **3,** 513–522.

MRI, 1992: A synthetic study on cloud-radiation processes (in Japanese). Tech. Rep. 29, MRI, 340 pp.

Nakajima, T., and M. D. King, 1990: Determination of the optical thickness and effective particle radius of clouds from reflected solar radiation measurements. Part I: Theory. *J. Atmos. Sci.*, **47,** 1878–1893.

Rawlins, F., and J. S. Foot, 1990: Remotely sensed measurements of stratocumulus properties during FIRE using the C130 aircraft multi-channel radiometer. *J. Atmos. Sci.*, **47,** 2488–2503.

Scott, J. C., and G. L. Stephens, 1984: A visible-infrared spectraradiometer for cloud reflectance measurements. *J. Phys. E,* **18,** 697–701.

Stephens, G. L., and J. C. Scott, 1985: A high speed spectrally scanning radiometer (SPERAD) for airborne measurements of cloud optical properties. *J. Atmos. Oceanic Technol.*, **2,** 148–156.

——, and C. M. R. Platt, 1987: Aircraft observations of the radiative and microphysical properties of stratocumulus and cumulus cloud fields. *J. Climate Appl. Meteor.*, **26,** 1243–1269.

Tanaka, T., T. Matsuo, K. Okada, I. Ichimura, S. Ichikawa, and A. Tokuda, 1989: An airborne video-microscope for measuring cloud particles. *Atmos. Res.*, **24,** 71–80.

Twomey, S., 1971: Radiative transfer: Terrestrial clouds. *J. Quant. Spectrosc. Radiat. Transfer,* **11,** 779–783.

——, and T. Cocks, 1989: Remote sensing of cloud parameters from spectral reflectance in the near-infrared. *Beitr. Phys. Atmos.*, **62,** 172–179.